# Slender-Body Aerodynamics for High-Speed Ground Vehicles

HENRY W. WOOLARD*
*Beta Technology Company, Palos Verdes Peninsula, Calif.*

**Classical slender-body theory for the prediction of the steady-state aerodynamic characteristics of high-speed ground vehicles of arbitrary cross section is presented. Special consideration is given to the effect of a side wind. The effectiveness of side fences in providing aerodynamic shielding from a side wind is treated in an approximate manner. Specific analytical relations and normalized parametric curves are presented for vehicles having similar semielliptic cross sections. The theory indicates that, for an unshielded vehicle, a side wind introduces a significant lift force which is proportional to the square of the yaw angle and the projected side area of the vehicle. For unshielded vehicles with a truncated aft end, the side force and rolling moment vary linearly with yaw angle, and to the first and three-halves powers of the aft-end area, respectively. The side force decreases and the rolling moment increases with decreasing vehicle height-to-width ratio. For smoothly closing aft ends, there is no side force or rolling moment. In general, small-to-moderate shielding is ineffective in reducing the lift due to side wind, small shielding is slightly effective and moderate shielding quite effective in reducing the rolling moment, and small-to-moderate shielding very effective in reducing the side force. Comparisons with some preliminary wind-tunnel tests on unshielded ground vehicles of semicircular cross section show fairly good agreement.**

## Nomenclature

$A$ = local cross-sectional area of a ground-vehicle body, $A = S/2$
$A_S$ = projected side area of ground vehicle
$b$ = local half-width of ground-vehicle body, $b = b(x)$
$c$ = local height of ground-vehicle body, $c = c(x)$
$\bar{c}$ = $c/c_\lambda$
$C_l$ = rolling-moment coefficient, $l/q_\infty A_m d_m$
$C_m$ = pitching-moment coefficient, $m/q_\infty A_m \lambda$
$C_n$ = yawing-moment coefficient, $n/q_\infty A_m d_m$
$C_p$ = pressure coefficient $(p - p_\infty)/q_\infty$
$C_Y$ = side-force coefficient, $Y/q_\infty A_m$
$C_Z$ = lift coefficient, $Z/q_\infty A_m$
$d_m$ = diameter of a circle of area $A_m$
$k$ = $(1 - \tau^2)$
$K_p{}^{(C)}$ = pressure coefficient $(p - p_\infty)/q_C$
$l,m,n$ = rolling, pitching, and yawing moments, respectively (see Fig. 1)
$n$ = outwardly directed normal to a body surface
$p$ = static pressure
$q_\infty, q_C$ = dynamic pressure, $\rho U_\infty{}^2/2$, $\rho V_C{}^2/2$
$S$ = local cross-sectional area of composite body, $S = S(x)$, $2A$
$S'$ = $dS/dx$
$u,v,w$ = total velocity components parallel to $x,y,z$, respectively
$u',v',w'$ = perturbation velocity components
$U_\infty$ = freestream velocity (see Fig. 1)
$V_C$ = cross-flow velocity, $U_\infty \beta$
$x,y,z$ = rectangular coordinates in body axes system
$y^*,z^*$ = nondimensional coordinates, $y/b$, $z/b$
$\hat{y},\hat{z}$ = nondimensional coordinates, $y/c$, $z/c$
$y_W$ = ordinate of projection of shield on body surface (see Fig. 3)
$Y,Z$ = side and normal (lift) forces; parallel to the $y$ and $z$ axes
$z_W$ = height of aerodynamic shield
$\beta$ = yaw angle (see Fig. 1)
$\gamma^2$ = $b^2 - c^2$
$\zeta$ = complex variable, $\zeta \equiv y + iz$
$\lambda$ = body length
$\nu$ = outwardly directed normal to a contour in $yz$ plane
$\xi$ = nondimensional shield height, $z_W/c_\lambda$
$\tau$ = $c/b$
$\Phi$ = $\varphi_\beta - V_C y$
$\varphi$ = perturbation velocity potential
$\varphi_S$ = see Eq. (7)
$(\ )_B$ = denotes the body surface
$(\ )_C, (\ )^{(C)}$ = due to side wind
$(\ )_m$ = body maximum cross-sectional area station
$(\ )_0, (\ )^{(0)}$ = due to body thickness
$(\ )_S, (\ )^{(S)}$ = associated with the potential, $\varphi_S$ (except $A_S$)
$(\ )_\lambda$ = denotes the aft end of the body
$(\ )_\beta, (\ )^{(\beta)}$ = due to side wind
$(\ )_\infty$ = denotes freestream conditions

Presented as Paper 70-139 at the AIAA 8th Aerospace Sciences Meeting, New York, January 19–21, 1970; submitted March 4, 1970; revision received September 14, 1970. Contributions of K. So, Rohr Corporation, Chula Vista, Calif., are acknowledged. This effort was supported in part by the Department of Transportation.

* President; presently Aerospace Engineer, Air Force Dynamics Laboratory, Wright-Patterson Air Force Base, Ohio. Associate Fellow AIAA.

## Introduction

STUDIES of ground vehicles designed to travel at speeds in the vicinity of 300 mph stem from an urgent need for a high-speed ground transportation system. Aerodynamic forces and moments can be sizable at these speeds and it is important to be able to predict these quantities accurately. This paper is concerned with the application of slender-body theory[1,2] to the prediction of the aforementioned aerodynamic characteristics, with particular emphasis on the effects of side winds. Slender-body theory is considered to be especially appropriate for this problem because of its capability for handling bodies of arbitrary cross section.

For tracked ground vehicles, some investigators have suggested guideways incorporating side walls or side fences to provide aerodynamic shielding and diminish the effects of side winds. In order to obtain an estimate of the effectiveness of aerodynamic shielding, the forces and moments for shielded vehicles are calculated herein on the assumption that the shielded portions of the vehicle are at freestream static pressure relative to side-wind flows. This admittedly does not conform to the actual flow. However, it is believed to provide a reasonably good approximation pending the availability of more definitive results.

The general theory for slender bodies of arbitrary cross section is outlined in the paper. Application, however, is limited to vehicles having similar semielliptic cross sections.

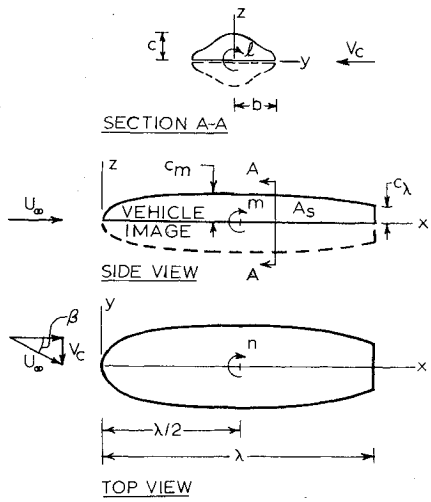


**Fig. 1 Illustration of notation.**

To the best of this writer's knowledge, there are no previous publications dealing with this subject.

## Analysis

### Slender-Body Boundary-Value Problem and Its Solutions

Analysis of the flow around a ground vehicle is accomplished by considering $\frac{1}{2}$ of the flow of an unbounded stream about the composite body formed by joining the ground-vehicle body to its ground-plane mirror image. The ground-plane boundary condition is thus automatically satisfied, the complication of determining a ground-plane potential is eliminated, and the analysis is transformed to the more conventional aerodynamics of bodies in free air.

The yawed flow about a composite body is shown in Fig. 1. The ground-vehicle body† of interest is the half-body lying above the $xy$ plane. The body cross-sectional shape is arbitrary except that it must be symmetric about the $y$ axis in order to satisfy the image requirement. Cross sections are assumed symmetrical about the $z$ axis also, since it is likely that most practical shapes will have this property.

The governing partial differential equation for a weakly disturbed subsonic or supersonic flow about a three-dimensional body is

$$(1 - M_\infty^2)\varphi_{xx} + \varphi_{yy} + \varphi_{zz} = 0 \tag{1}$$

where $M_\infty$ is the freestream Mach number, $x$, $y$, and $z$ are body oriented coordinates (Fig. 1), and $\varphi$ is the perturbation velocity potential. The perturbation velocity components are given by $u' = \varphi_x$, $v' = \varphi_y$, and $w' = \varphi_z$. The total velocity components are

$$u = u' + U_\infty, \quad v = v' - V_C, \quad w = w' \tag{2}$$

With appropriate assumptions regarding body slenderness and smoothness (see Ref. 1, p. 196), the first term in Eq. (1) may be neglected, and the governing equation becomes

$$\varphi_{yy} + \varphi_{zz} = 0 \tag{3}$$

It may be concluded, then, that the perturbation potential has the form, $\varphi = \varphi_{2D}(y,z;x) + \varphi_S(x)$, where $\varphi_{2D}(y,z;x)$ is a velocity potential for two-dimensional flow in a $yz$-plane, in which $x$ appears only as a parameter introduced by the geometry of the body cross section at $x$. Since the boundary conditions and governing equation are linear, it is convenient to separate $\varphi_{2D}$ into two components, so that the potential $\varphi$ becomes

$$\varphi = \varphi_S(x) + \varphi_0(y,z;x) + \varphi_\beta(y,z;x) \tag{4}$$

The potentials $\varphi_0$ and $\varphi_\beta$ are due to body thickness and yaw angle, respectively, and respectively satisfy the boundary conditions

$$-U_\infty \cos(n,x) = \partial\varphi_0/\partial\nu \tag{5}$$

$$V_C \cos(\nu,y) = \partial\varphi_\beta/\partial\nu \tag{6}$$

The flow problem specified by Eqs. (3) and (6) has been extensively treated in the classical literature of hydro- and aerodynamics. Solutions are available for arbitrary cross-sectional shapes and a variety of particular shapes having possible applicability to high-speed ground vehicles. The problem specified by Eqs. (3) and (5) is more difficult and has received little attention in the literature. It is likely that a formalized solution for bodies of arbitrary cross section can be achieved by conformal mapping methods. The only solutions currently known to the writer are for bodies of elliptic cross section[3] and a special shape derived by Graham.[4]

For a given body shape, it is apparent, from Eqs. (3, 5, and 6) that the solutions for $\varphi_o$ and $\varphi_\beta$ are independent of whether the flow is subsonic or supersonic. This permits the interchange of solutions previously obtained for either flow regime.

The potential $\varphi_S(x)$ accounts for the upstream and downstream propagation of pressure disturbances and therefore has different forms for subsonic and supersonic flow. For subsonic flow[1,2]

$$\varphi_S(x) = \frac{U_\infty S'(x)}{4\pi} \log \frac{1 - M_\infty^2}{4x(\lambda - x)} + \frac{U_\infty}{4\pi} \int_0^\lambda \frac{S'(x) - S'(\xi)}{|x - \xi|}\, d\xi \tag{7}$$

The potentials $\varphi_S$ and $\varphi_0$ are responsible for the forward-speed body lift. The slender-body solutions for these potentials are inapplicable at the ends of bodies having rounded fore and aft ends or to bodies having a truncated aft end, all likely possibilities for high-speed ground vehicles. Although the problem of handling these geometries has not been investigated in depth in this study, an approximate method for treating rounded ends is advanced. Since, for highly elongated bodies, the lift contribution of regions at rounded ends is likely to be relatively small, a suggested tentative procedure is to formally apply the slender-body method, but omit a small region at the ends in integrating the surface pressures for the vehicle lift. This procedure requires a method for uniquely determining the extent of the region to be omitted. The following result suggests a criterion. From exact relations for axial flow about an ellipsoid of revolution, it can be shown in the limiting case of a highly elongated ellipsoid that the associated source distribution lies only between the ellipsoid foci. Since slender-body theory relates a source distribution to the local body slope, this result suggests that the regions between the foci and the ends are the appropriate ones to omit in the aforementioned integration. For rounded ends on nonelliptic bodies of revolution and bodies of arbitrary cross section, the focus of the osculating ellipsoid is used.

In order to estimate the error incurred in neglecting the end lift, these contributions were determined for the exact axial flow about an ellipsoid of revolution (prolate spheroid). The resulting relative error for the half-body lift for several half-body thickness ratios is given in Table 1. It can be seen from the table that neglect of the end lift is an acceptable en-

**Table 1 Lift error due to end lift**

| $c_m/\lambda$ | 0.10 | 0.20 | 0.25 | 0.30 |
|---|---|---|---|---|
| $\Delta C_Z/C_Z$ | 0 | −0.03 | −0.06 | −0.11 |

† Hereinafter, the composite body will be referred to as the "body" and the ground-vehicle body as the "half-body," "vehicle body," or "ground-vehicle body."

gineering approximation for half-body thickness ratios below 0.25.

The exact and slender-body lift coefficients for axial flow about a prolate spheroid half body are shown in Fig. 2 as functions of half-body thickness ratio. It is seen that the slender-body value begins to diverge rapidly from the exact result for values of the thickness ratio, $c_m/\lambda$, in excess of 0.10. From this comparison, it would appear that application of slender-body theory to the calculation of the axial flow lift should be restricted to vehicle body thickness ratios below 0.10.

### Pressure Coefficient

The pressure coefficient in a body coordinate system is given by

$$C_p = -2\frac{u'}{U_\infty} + 2\beta\frac{v'}{U_\infty} - \left(\frac{v'}{U_\infty}\right)^2 - \left(\frac{w'}{U_\infty}\right)^2 \quad (8)$$

where

$$u' = u_S' + u_0' + u_\beta' \quad (9)$$

$$v' = v_0' + v_\beta',\ w' = w_0' + w_\beta' \quad (10)$$

and $v_S'$ and $w_S'$ are nonexistent, and the subscripts denote contributions due to the corresponding potentials.

In the process of calculating section forces and moments ($dC_Z/dx$, $dC_l/dx$, etc.) by integration of surface-pressure coefficients, the following pressure-coefficient combinations occur

$$(C_p)_L \pm (C_p)_R \quad (11)$$

where $(C_p)_L$ and $(C_p)_R$ represent $C_p(-y,z)$ and $C_p(y,z)$, respectively.

In constructing the pressure coefficient combinations given by (11), it is convenient to make use of the symmetric and antisymmetric properties of the velocity potentials and their velocity components. From inspection, it may be deduced that $u_S'$, $u_0'$, $w_0'$, and $v_\beta'$ are symmetric with respect to the $z$ axis, and $v_0'$, $u_\beta'$, $w_\beta'$, $(v_0'v_\beta')$, and $(w_0'w_\beta')$ are antisymmetric with respect to the $z$ axis.

Making use of Eqs. (2, 8–10) and the symmetric and antisymmetric properties of the velocity components, we obtain

$$C_p = K_p^{(S)} + K_p^{(0)} + \beta^2 K_p^{(C)} + \beta k_p^{(\beta)} + \beta k_p^{(x)} \quad (12)$$

where

$$K_p^{(S)} \equiv -2\left(\frac{u_S'}{U_\infty}\right) \quad (13)$$

$$K_p^{(0)} \equiv -2\left(\frac{u_0'}{U_\infty}\right) - \left(\frac{v_0'}{U_\infty}\right)^2 - \left(\frac{w_0'}{U_\infty}\right)^2 \quad (14)$$

$$K_p^{(C)} \equiv 1 - \left(\frac{V_\beta}{V_C}\right)^2 - \left(\frac{w_\beta}{V_C}\right)^2 \quad (15)$$

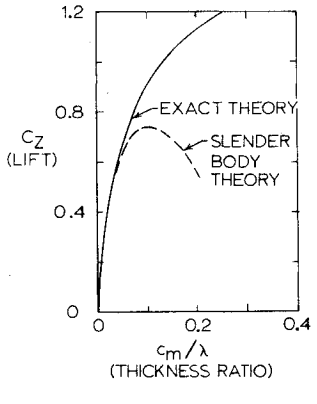


**Fig. 2 Exact and slender-body axial-flow lift coefficient for a prolate spheroid half body.**

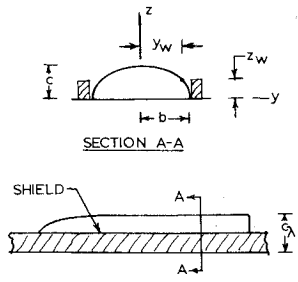


**Fig. 3 Aerodynamic shield.**

$$k_p^{(\beta)} \equiv -2\left(\frac{u_\beta'}{V_C}\right) \quad (16)$$

$$k_p^{(x)} \equiv -2\left(\frac{v_0'}{U_\infty}\right)\left(\frac{v_\beta}{V_C}\right) - 2\left(\frac{w_0'}{U_\infty}\right)\left(\frac{w_\beta}{V_C}\right) \quad (17)$$

In the foregoing relations, the upper case and lower case coefficients are symmetric and antisymmetric, respectively, with respect to $z$. The superscripts, $S$, 0, and $\beta$, denote contributions from the velocity potentials, $\varphi_S$, $\varphi_0$, and $\varphi_\beta$, respectively. The coefficient, $K_p^{(C)}$, is also due to $\varphi_\beta$, and has the form $(p - p_\infty)/qc$. The superscript $x$ denotes a cross-coupling contribution.

The expression from (11) can now be written in equation form as

$$(C_p)_L - (C_p)_R = 2\beta(k_p^\beta)_R + 2\beta(k_p^x)_R \quad (18)$$

$$(C_p)_L + (C_p)_R = 2(K_p^S)_R + 2(K_p^0)_R + 2\beta^2(K_p^C)_R \quad (19)$$

### Section Force and Moment Coefficients

Allowing for the symmetric and antisymmetric properties of the pressure coefficient, and integrating over the unshielded portions of the vehicle body, the section force and moment coefficients are

$$\frac{dC_Z}{dx} = \frac{-1}{A_m}\int_0^{y_W}[(C_p)_L + (C_p)_R]dy \quad (20)$$

$$\frac{dC_Y}{dx} = \frac{1}{A_m}\int_{z_W}^{c}[(C_p)_L - (C_p)_R]dz \quad (21)$$

$$\frac{dC_l}{dx} = \frac{-1}{A_m d_m}\int_0^{y_W}[(C_p)_L - (C_p)_R]y\,dy + \frac{1}{A_m d_m}\int_{z_W}^{c}[(C_p)_L - (C_p)_R]z\,dz \quad (22)$$

where, $y_w$ and $z_w$ are defined in Fig. (3). All the total coefficients, including the pitching and yawing moment coefficients, are obtainable from these quantities.

Section force and moment coefficients can also be written as

$$dC_Z/dx = (dC_Z/dx)^{(S)} + (dC_Z/dx)^{(0)} + (dC_Z/dx)^{(C)} \quad (23)$$

$$dC_Y/dx = (dC_Y/dx)^{(\beta)} + (dC_Y/dx)^{(x)} \quad (24)$$

$$dC_l/dx = (dC_l/dx)^{(\beta)} + (dC_l/dx)^{(x)} \quad (25)$$

where each component of a section coefficient is related to the corresponding integral resulting from the substitution of Eq. (18) or (19) in Eqs. (20–22). It should be noted that shielding is not allowed to influence the first two terms on the right hand side of Eq. (23). The upper limit on the integrals is taken as $b$ for these contributions.

## Application

### Ground Vehicles with Semielliptic Cross Sections

Ground vehicles having semielliptic cross sections will be considered now. The semielliptic section allows for convenient delineation of the effects of height-to-width ratio. In addition, it is believed to represent a practical geometry

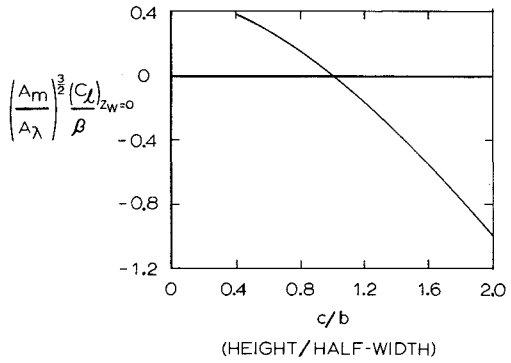


**Fig. 4 Normalized rolling-moment coefficient due to side wind for unshielded bodies with similar semielliptic cross sections.**

for high-speed ground vehicles, even though its selection was based on the availability of the appropriate flow solutions.

The potential $\varphi_0$ for bodies having a longitudinal distribution of similar elliptic cross sections is available several places in the technical literature. Kahane and Solarski,[3] however, have obtained a more general solution valid also for a distribution of nonsimilar elliptic sections. Considerations here are restricted to similar cross sections, since the nonsimilar relations are cumbersome, and because, as far as aerodynamic shielding effects are concerned, the results are qualitatively alike for the two situations.

Adapting the potential $\varphi_0$ of Kahane and Solarski[3] to the present problem, there is obtained

$$\varphi_0 = [U_\infty S'(x)/4\pi \cosh^{-1}] \{\pm[(y^2 + z^2)/\gamma^2] \pm (J)^{1/2}\} + [U_\infty S'(x)/4\pi] \log(|\gamma^2|/4) \quad (26)$$

where

$$J \equiv \{[(y^2 + z^2)/\gamma^2] + 1\}^2 - 4y^2/\gamma^2 \quad (27)$$

The upper signs are taken for $b > c$ and the lower ones for $b < c$.

The potential $\varphi_\beta$ is available many places in the technical literature (e.g., see Ref. 5, p. 156). It is most conveniently presented in terms of the classical complex potential $W_\beta$ ($W_\beta \equiv \Phi_\beta + i\Psi_\beta$). This potential is

$$W_\beta = -(V_C/2)[\zeta + (\zeta^2 - \gamma^2)^{1/2}] - (V_C/2)[(1 + \tau)/(1 - \tau)][\zeta - (\zeta^2 - \gamma^2)^{1/2}] \quad (28)$$

In considering the contribution of a side wind to the section coefficients defined in Eqs. (18–25), inspection of Eqs. (19) and (20) indicates that there is no side-wind contribution to $(dC_Z/dx)^{(s)}$ and $(dC_Z/dx)^{(0)}$. Therefore, the pertinent velocity components required for the determination of the affected section coefficients are

$$(v_0'/U_\infty)_B = [S'(x)/2\pi b]\, \tau y^*/(1 - ky^{*2}) \quad (29)$$

$$(w_0'/U_\infty)_B = [S'(x)/2\pi b](1 - y^{*2})^{1/2}/(1 - ky^{*2}) \quad (30)$$

$$(u_\beta'/V_C)_B = -(1 + \tau)\tau^2(db/dx)y^*/(1 - ky^{*2}) \quad (31)$$

$$(v_\beta/V_C)_B = -(1 + \tau)(1 - y^{*2})/(1 - ky^{*2}) \quad (32)$$

$$(v_\beta'/V_C)_B = (v_\beta/V_C) + 1 \quad (33)$$

$$(w_\beta'/V_C)_B = \tau(1 + \tau)y^*(1 - y^{*2})^{1/2}/(1 - ky^{*2}) \quad (34)$$

The preceding relations may be written in terms of the variable $z$ by utilizing the equation for an ellipse.

If Eqs. (29–34) are substituted in the appropriate relations, the integrations in Eqs. (20–22) may be performed (with change of variable where required) and the corresponding section coefficients obtained.

The cross-coupling section coefficients were found to be zero. Of the three remaining section coefficients, the side force and rolling moment are integratable with respect to $x$ for a constant shield height. These total coefficients are therefore independent of the body longitudinal area distribution. The total lift coefficient, on the other hand, depends on the specific area distribution of the body.

The following relations are obtained for the section lift coefficient and the total side force and rolling moment coefficients, respectively.

$$\frac{A_m}{b\beta^2}\left(\frac{dC_Z}{dx}\right)^{(C)} = -2\tau\left(\frac{1+\tau}{1-\tau}\right)\left(1 - \frac{\xi^2}{\bar{c}^2}\right)^{1/2} \times \left(\frac{\tau \tanh^{-1}\{k[1 - (\xi/\bar{c})^2]\}^{1/2}}{\{k[1 - (\xi/\bar{c})^2]\}^{1/2}} - \frac{2}{1+\tau}\right) \quad (35)$$

$$\left(\frac{A_m}{A_\lambda}\right)\frac{C_Y}{\beta} = -2\delta\tau\pi\left[1 + \left(\frac{1+\tau}{\tau^2}\right)\xi^2\right] + 4\delta\left(\frac{1+\tau}{\tau}\right)\left[\tau\xi(1 - \xi^2)^{1/2} + \xi^2 \cot^{-1}\left(\frac{\tau(1 - \xi^2)^{1/2}}{\xi}\right)\right] + \delta\left(\frac{4\tau}{1-\tau}\right)\left[\cot^{-1}\left(\frac{\tau(1 - \xi^2)^{1/2}}{\xi}\right) - \tau \cot^{-1}\left(\frac{(1 - \xi^2)^{1/2}}{\xi}\right)\right] \quad (36)$$

$$\left(\frac{A_m}{A_\lambda}\right)^{3/2}\frac{C_l}{\beta} = \delta(1+\tau)\frac{4(2\tau)^{1/2}}{3\pi}\left[\frac{\tanh^{-1}[k(1 - \xi^2)]^{1/2}}{(k)^{1/2}} + \frac{(1 - \tau^2)}{\tau^3}\xi^3 \tan^{-1}\left(\frac{\tau(1 - \xi^2)^{1/2}}{\xi}\right) - (\xi/\tau)^2(1 - \xi^2)^{1/2} - (1 - \xi^2)^{3/2}\right] \quad (37)$$

for $c(0) = 0$. The parameter $\delta$ is taken as $\delta = 1.0$ for ($\xi < 1.0$) and as $\delta = 0$ for ($\xi \geq 1.0$).

The foregoing results are valid for $\tau \gtrless 1.0$, where for positive $B$, use is made of the relation, $(-B)^{-1/2}\tanh^{-1}(-B)^{1/2} = (B)^{-1/2}\tan^{-1}(B)^{1/2}$.

The indeterminate forms encountered in Eqs. (35) and (36) for a semicircular vehicle cross section ($\tau = 1.0$) may be evaluated by L'Hospital's rule.

Before considering the effect of aerodynamic shielding as given by Eqs. (35–37) it is of interest to examine the aerodynamic characteristics of the unshielded vehicle.

Inspection of Eq. (35) for zero shield height reveals that, to a very good approximation, the section lift coefficient due to a side wind is given by

$$(dC_Z/dx)_{Z_W=0}{}^{(C)} \cong (10/3)(b/A_m)(c/b)\beta^2 \quad (0 \leq c/b \leq 2.0) \quad (38)$$

The greatest deviation of the above relation from the exact

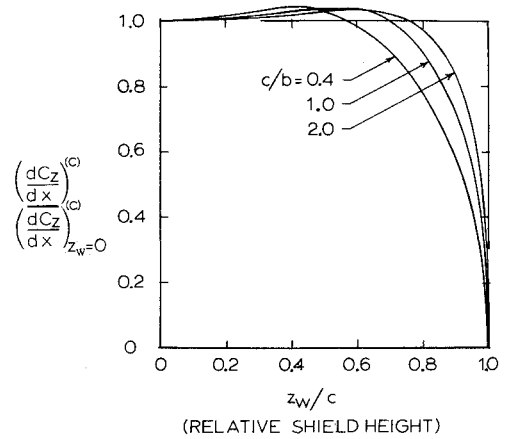


**Fig. 5 Effect of shield height on the section-lift coefficient due to side wind for semielliptic cross section bodies.**

result, given by Eq. (35) occurs at $(c/b) = 0.3$, at which point the relative error is 6%. For all other values of $c/b$, the error is considerably smaller.

Integrating Eq. (38) with the condition $c(0) = 0$, and letting $\xi = 0$ in Eqs. (36) and (37) gives the following respective relations for the coefficients of lift, side force, and rolling moment due to a side wind

$$(C_Z)_{z_W=0}{}^{(C)} = (10/3)(A_S/A_m)\beta^2 \quad (39)$$

$$(C_Y)_{z_W=0} = -2(A_\lambda/A_m)\tau\beta \quad (40)$$

$$(C_l)_{z_W=0} = \frac{16}{3\pi}\left(\frac{A_\lambda}{A_m}\right)^{3/2}\left(\frac{\tau}{2}\right)^{3/2}(1+\tau)\times \left[\frac{\tanh^{-1}(1-\tau^2)^{1/2}}{(1-\tau^2)^{1/2}} - 1\right]\beta \quad (41)$$

where $\tau \equiv c/b$.

Equations (39–41) indicate that, for a given vehicle, the lift varies as the square of the yaw angle whereas the side force and rolling moment vary linearly with yaw angle. For unshielded vehicles, the lift due to a side wind may be reduced by decreasing the projected side area, $A_S$. For a fixed vehicle height-to-half-width ratio, $\tau$, the side force and rolling moment may be reduced by decreasing the vehicle aft-end area, $A_\lambda$. For a closed aft end ($A_\lambda = 0$), there is no side force or rolling moment. For a fixed aft-end area, it is apparent from Eq. (40) that the side force can be lowered by reducing the vehicle height-to-half-width ratio. A normalized plot of the rolling moment calculated from Eq. (41) is given in Fig. 4. This plot shows that for a fixed value of $A_\lambda$ the rolling moment is zero for a semicircular cross section ($c/b = 1.0$), increases positively with decreasing height-to-half-width ratio, and increases negatively for an increasing height-to-half-width ratio. Therefore, although reduction of the vehicle height-to-half-width ratio to values below unity favorably influences the side force, it adversely affects the rolling moment.

The effect of shield height on the section-lift coefficient due to side wind is shown in Fig. 5. Although the degree of influence varies with vehicle height-to-half-width ratio, shielding is generally rather ineffective in reducing this lift contribution. Shield height-to-body height ratios in excess of 0.8 are required in order to achieve any substantial lift reduction. Small relative shield heights actually increase the lift slightly due to the fact that the area shielded includes a cross-flow stagnation region.

The shielding effect on side force is shown in Fig. 6. Although there is a secondary influence of body height-to-half-width ratio, small-to-moderate relative shield heights generally are very effective in reducing the side force. This effectiveness (i.e., the rate of reduction with height) is considerably lessened at greater shield heights where the side force is small.

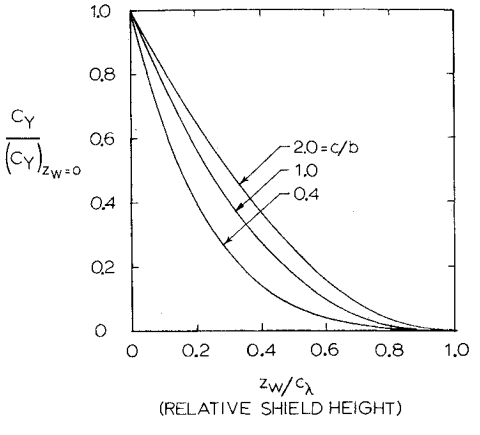


**Fig. 6 Effect of shield height on the side force due to side wind for bodies with similar semielliptic cross sections.**

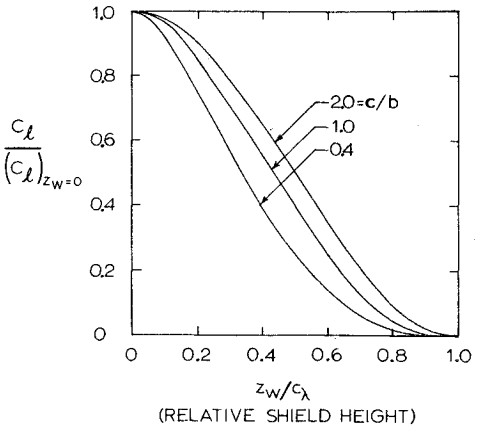


**Fig. 7 Effect of shield height on the rolling moment due to side wind for bodies with similar semielliptic cross sections.**

The effect of shield height on rolling moment is shown in Fig. 7. Although once again there is a secondary influence of body height-to-half-width ratio, it can be concluded from the figure that small relative shield heights ($z_W/c_\lambda < 0.15$) are slightly effective and moderate heights are quite effective in reducing the rolling moment due to side wind.

## Comparison with Experiment

Kalman J. Grunwald of the NASA Langley Research Center has conducted preliminary wind-tunnel tests on several unshielded ground-vehicle body shapes. A comparison of the theoretical prediction of side-wind effects with experimental results‡ for one of the models tested by Grunwald is made in this section.

Model tests were conducted in a moving-ground-plane wind tunnel at an air speed of approximately 100 fps, both with ground plane stopped and moving. The principal differences in aerodynamic characteristics due to the mode of ground-plane operation occurred in the pitching moment and drag coefficients at low heights. The other aerodynamic coefficients were affected only slightly by a change in ground-plane conditions.

The model selected for comparison is 72 in. long having a semicircular cross section with 6.4 in. radius, an elliptic nose with a 28 in. semimajor axis, and a truncated aft end. Test results are presented for a height of 0.1 in. above the ground. All experimental coefficients presented here, except the pitching-moment coefficient, are an average of the ground-plane-moving and the ground-plane-stopped results.

The moment coefficients are presented in Figs. 8 as a function of the experimentally measured yaw angle. (There are indications here and in subsequent data of approximately −1.5–2.5° yaw instrument misalignment. The experimental yaw angle presented is therefore designated as an uncorrected angle.)

Although simple geometric considerations for a semicircular cross section indicate that there should be no rolling moment due to the external flow, the data plotted in Fig. 8 shows that a rolling moment was experienced. This moment is attributed to a lateral pressure distribution across the bottom of the model. A theoretical estimate of its magnitude was made by assuming the aforementioned lateral pressure distribution to be linear at a given longitudinal station with the pressure at the edges calculated from slender-body theory. On this basis, the rolling-moment contribution was found to

‡ The test data used are documented in a NASA Working Paper of limited distribution.

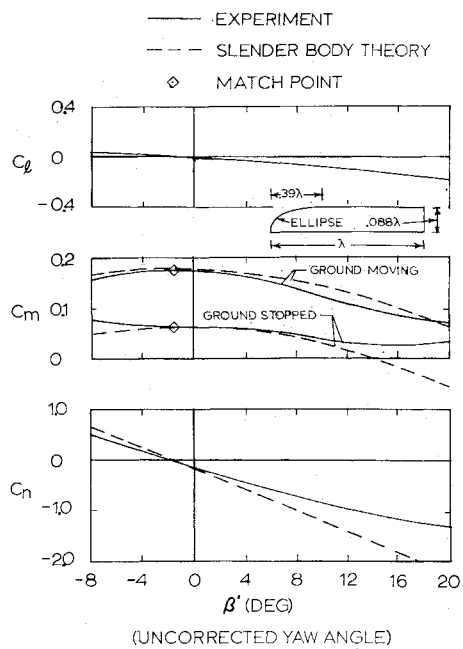


**Fig. 8 Comparison of experimental and theoretical moment coefficients.**

be given by $C_l = -8(2)^{1/2}\beta/9\pi$. When adjusted for the experimental yaw misalignment, this relation gives excellent agreement with the experimental curve shown in Fig. 8.

The theoretical zero-yaw pitching moment and lift coefficients were not calculated for this model. The pitching moment involves a knowledge of the bottom flow as well as the external flow, and the truncated aft end presents a difficulty in the lift calculation. In any case, side-wind effects are the main consideration here. In comparing theory and experiment, therefore, the theoretical curves for pitching moment and lift are matched to the experimental values at zero yaw angle (with experiment corrected for alignment error).

Theoretical predictions of the incremental pitching moment due to yaw shown in Fig. 8 are considered fair. The yawing-moment agreement with experiment is of marginal acceptability at low yaw angles and diverges unacceptably at the higher angles. Comparisons of force coefficients calculated from slender-body theory and measured experimentally are shown in Fig. 9. Agreement is considered good for both the side-force coefficient and the incremental lift coefficient even at rather large yaw angles.

## Concluding Remarks

In the application of slender-body theory to the aerodynamics of high-speed ground vehicles having similar semielliptic cross sections, it has been determined that for an unshielded vehicle a side wind introduces a significant lift force which is proportional to the square of the yaw angle and the projected side area of the vehicle. For unshielded

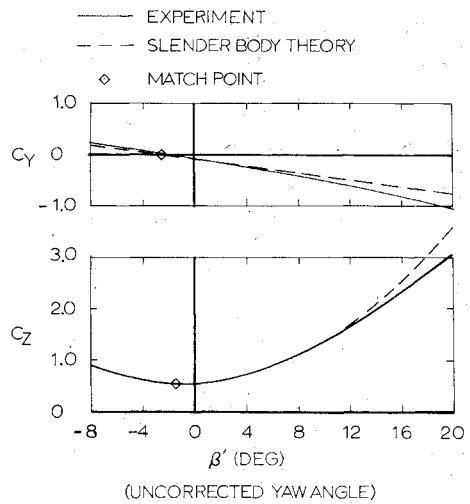


**Fig. 9 Comparison of experimental and theoretical force coefficients.**

vehicles with a truncated aft end, the side force and rolling moment vary linearly with yaw angle, and to the first and three-halves powers of the aft-end area, respectively. The side force decreases and the rolling moment increases with decreasing vehicle height-to-width ratio. For smoothly closing aft ends, there is no side force or rolling moment. In general, small-to-moderate shielding is ineffective in reducing the lift due to side wind, small shielding is slightly effective and moderate shielding quite effective in reducing the rolling moment, and small-to-moderate shielding very effective in reducing the side force.

On the basis of limited comparisons between theory and experiment for unshielded ground vehicles of semicircular cross section, it appears that slender-body theory is capable of yielding fairly good engineering estimates of the aerodynamic forces due to side wind for high-speed ground vehicles. It is likely that better agreement could be achieved by incorporating refinements which include viscous effects, vortex shedding, and other phenomena. Additional comparisons with experiment are required in order to assess the capabilities of the theory more confidently.

## References

[1] *Ward, G. N., Linearized Theory of Steady High-Speed Flow,* Cambridge University Press, 1955.

[2] Ashley, Holt, and Landahl, Martin, *Aerodynamics of Wings and Bodies,* Addison-Wesley, Reading, Mass., 1965, pp. 99–119.

[3] Kahane, A. and Solarski, A., "Supersonic Flow about Slender Bodies of Elliptic Cross Section," *Journal of the Aeronautical Sciences,* Vol. 20, No. 8, Aug. 1953, pp. 513–524.

[4] Graham, E. W., "The Pressure on a Slender Body of Nonuniform Cross-Sectional Shape in Axial Supersonic Flow," *Journal of the Aeronautical Sciences,* Vol. 17, No. 3, March 1950, pp. 173–175, 192.

[5] Milne-Thomson, L. M., *Theoretical Hydrodynamics,* Macmillan, New York, 1938.